Vol 18 No 7, July 2009
1674-1056/2009/18(07)/2680-10

Chinese Physics B

© 2009 Chin. Phys. Soc.
and IOP Publishing Ltd

A novel four-wing chaotic attractor generated from a three-dimensional quadratic autonomous system*

Dong En-Zeng(董恩增)[a)†], Chen Zai-Ping(陈在平)[a)],
Chen Zeng-Qiang(陈增强)[b)], and Yuan Zhu-Zhi(袁著祉)[b)]

[a)] *Department of Automation, Tianjin University of Technology, Tianjin* 300484, *China*

[b)] *Department of Automation, Nankai University, Tianjin* 300071, *China*

(Received 12 December 2008; revised manuscript received 16 March 2009)

This paper presents a new 3D quadratic autonomous chaotic system which contains five system parameters and three quadratic cross-product terms, and the system can generate a single four-wing chaotic attractor with wide parameter ranges. Through theoretical analysis, the Hopf bifurcation processes are proved to arise at certain equilibrium points. Numerical bifurcation analysis shows that the system has many interesting complex dynamical behaviours; the system trajectory can evolve to a chaotic attractor from a periodic orbit or a fixed point as the proper parameter varies. Finally, an analog electronic circuit is designed to physically realize the chaotic system; the existence of four-wing chaotic attractor is verified by the analog circuit realization.

Keywords: chaos, four-wing chaotic attractor, bifurcation analysis, chaotic circuit
PACC: 0545

1. Introduction

Since Lorenz proposed the first chaotic system,[1] much progress has been made on chaos theory, for example, the dynamical properties of chaotic systems have been thoroughly studied.[2−7] Recently, the research focus of chaotic dynamical systems is mainly on the engineering application, furthermore, many great achievements have been made in the field of secure communication and information encryption.[8−10] Therefore, the generation of complex chaotic system becomes a hot topic. Based on the Lorenz system, Chen and Ueta[11] presented the Chen system by using the chaos anti-control method. After that, Lü *et al* [12,13] proposed Lü system and Lorenz system family. Qi *et al* [14] proposed a 3D two-wing chaotic system through adding a nonlinear quadratic term into the Lorenz system. Liu *et al* [15] proposed a 3D autonomous chaotic system, which can generate a new butterfly-shaped attractor. Li and Song[16] realized chaos anti-control of nonlinear systems based on the sliding mode variable structure control method. Wang *et al* [17] presented a 4D chaotic system with multi-scroll attractors.

Liu and Chen[18] firstly proposed a 3D four-wing chaotic system, but in Ref.[19] they proved the impossibility of having a single four-wing chaotic attractor in this system. Chen *et al* [20] proposed a 3D autonomous chaotic system which can generate a single four-wing attractor and a single three-wing attractor under proper parameter conditions. Qi *et al* [21] also proposed a 3D autonomous chaotic system that can generate a pair of diagonal double-wing attractors.

By utilizing the chaotic anti-control method, this paper presents a new 3D quadratic autonomous chaotic system, which contains five parameters and three quadratic cross-product terms. Compared with the Lorenz system family, the proposed system has a different algebraic structure and can generate a single four-wing chaotic attractor. The system is proved to undergo Hopf bifurcations at certain equilibrium points. Numerical bifurcation analysis shows that the system has many complex dynamical behaviours. Finally, an analog circuit is designed to physically realize the chaotic system; the existence of the four-wing chaotic attractor is verified by the analog circuit realization.

*Project supported by the National Natural Science Foundation of China(Grant Nos 60774088 and 10772135), the Foundation of the Application Base and Frontier Technology Research Project of Tianjin, China (Grant Nos 07JCZDJC09600, 08JCZDJC21900 and 08JCZDJC18600) and the Tianjin Key Laboratory for Control Theory & Applications in Complicated Industry Systems of China.

†Corresponding author. E-mail: dongenzeng@163.com

2. A new four-wing chaotic system

The pseudo four-wing chaotic system, which is presented by Liu and Chen,[18] can be described as follows:

$$\begin{aligned}\dot{x} &= ax - yz,\\ \dot{y} &= -by + xz\\ \dot{z} &= -cz + xy. \end{aligned} \tag{1}$$

By introducing a positive linear state feedback term in the third equation of system (1), a new 3D autonomous chaotic system is given by

$$\begin{aligned}\dot{x} &= ax - byz,\\ \dot{y} &= -cy + xz,\\ \dot{z} &= kx - dz + xy, \end{aligned} \tag{2}$$

where a, b, c, d, $k \in R^+$. The new system (2) can be chaotic with wide parameter ranges and has many interesting complex dynamic behaviours. Let

$$\begin{aligned} x_2 &= -\frac{1}{2a}(k\sqrt{bac} - \sqrt{back^2 + 4a^2dc}),\\ y_2 &= -\frac{1}{2b}(k - \sqrt{b^2k^2 + 4abd}),\\ z_2 &= \frac{1}{b}\sqrt{bac},\\ x_4 &= -\frac{1}{2a}(k\sqrt{bac} + \sqrt{back^2 + 4a^2dc}),\\ y_4 &= -\frac{1}{2b}(k + \sqrt{b^2k^2 + 4abd}),\\ z_4 &= \frac{1}{b}\sqrt{bac}, \end{aligned}$$

then the five equilibrium points of the system (2) can be described as follows:

$$\begin{aligned} S_1 &= (0, 0, 0),\\ S_2 &= (x_2, y_2, z_2),\\ S_3 &= (-x_2, y_2, -z_2),\\ S_4 &= (x_4, y_4, z_4),\\ S_5 &= (-x_4, y_4, -z_4). \end{aligned}$$

When $a > 0$, $b > 0$, $c > 0$, $d > 0$, $k > 0$, the system always has five equilibrium points while generalized Lorenz canonical form (GLCF) has three equilibrium points, thus they are topologically inequivalent.

2.1. Stability of the chaotic system

When $b > 1$, $c > 0$, $d > 0$, $k > 0$ and $a < -\dfrac{k^2}{4d}$, let the Lyapunov function be

$$V(x, y, x) = \frac{1}{2}(x^2 + (b-1)y^2 + z^2). \tag{3}$$

Then

$$\begin{aligned} \dot{V}(x, y, z) &= x\dot{x} + (b-1)y\dot{y} + z\dot{z}\\ &= a\left(x^2 + \frac{k}{a}xz + \frac{k^2}{4a^2}z^2\right)\\ &\quad - c(b-1)y^2 - \left(d + \frac{k^2}{4a}\right)z^2\\ &= a\left(x + \frac{k}{2a}z\right)^2 - c(b-1)y^2\\ &\quad - \left(d + \frac{k^2}{4a}\right)z^2 < 0. \end{aligned}$$

Thus the zero equilibrium of the system (2) is globally asymptotically stable.

2.2. Dissipativity and existence

Under the condition that $c > 0$, $d > 0$, and $a < 0$, we have

$$\nabla V = \frac{\partial \dot{x}}{\partial x} + \frac{\partial \dot{y}}{\partial y} + \frac{\partial \dot{z}}{\partial z} = -(c + d - a). \tag{4}$$

According to the ranges of the system parameters, we obtain that $-(c + d - a) < 0$, and thus the system is a dissipative system. All orbits of the system converge to a specific subset of zero volume as $t \to \infty$ exponentially

$$\frac{\mathrm{d}V}{\mathrm{d}t} = \mathrm{e}^{-(c+d-a)}. \tag{5}$$

It is known that a volume element with its initial volume being $V(0)$ can shrink to $V_0\mathrm{e}^{-(c+d-a)t}$, indicating that every volume element can shrink to 0 with the exponential speed $-(c+d-a)$. All the system orbits can be limited to a point set of which the volume is 0, and its asymptotic dynamical behaviour can be fixed on an attractor.

2.3. Symmetry and similarity

Obviously, system (2) is symmetric with respect to the y-axis, which can be easily proved via the coordinate transform $(x, y, z) \to (-x, y, -z)$.

Equilibrium points S_2 and S_3 are symmetric with respect to the y-axis. The same holds for S_4 and S_5. But under the coordinate transformation $(x, y, z) \to (-x, -y, z)$, $(x, y, z) \to (x, -y, -z)$ and $(x, y, z) \to (-x, -y, -z)$, the system is not the same as the original system; this means that the system can show more complex dynamical behaviours.

The equilibrium points S_2 and S_3 have the same eigenvalues; the eigenvalues of S_4 and S_5 are also the same, but not the same as those of S_2 and S_3.

To verify this, let J_i denote the Jacobian matrix of S_i, $i = 2, \ldots, 5$, namely,

$$\boldsymbol{J}_2 = \begin{bmatrix} a & -bz_2 & -by_2 \\ z_2 & -c & x_2 \\ k + y_2 & x_2 & -d \end{bmatrix}, \tag{6}$$

$$\boldsymbol{J}_3 = \begin{bmatrix} a & bz_2 & -by_2 \\ -z_2 & -c & -x_2 \\ k + y_2 & -x_2 & -d \end{bmatrix}, \tag{7}$$

$$\boldsymbol{J}_4 = \begin{bmatrix} a & -bz_4 & -by_4 \\ z_4 & -c & x_4 \\ k + y_4 & x_4 & -d \end{bmatrix}, \tag{8}$$

$$\boldsymbol{J}_5 = \begin{bmatrix} a & bz_4 & -by_4 \\ -z_4 & -c & -x_4 \\ k + y_4 & -x_4 & -d \end{bmatrix}. \tag{9}$$

There exists a matrix $\boldsymbol{T}$, such that

$$\boldsymbol{T}^{-1}\boldsymbol{J}_2\boldsymbol{T} = \boldsymbol{J}_3, \tag{10}$$

$$\boldsymbol{T}^{-1}\boldsymbol{J}_4\boldsymbol{T} = \boldsymbol{J}_5, \tag{11}$$

where $\boldsymbol{T} = \mathrm{diag}(-1, 1, -1)$, which is an orthogonal matrix,

$$\boldsymbol{T}^{-1} = \boldsymbol{T}^{\mathrm{T}} = \boldsymbol{T}. \tag{12}$$

Therefore, S_2, S_3 and S_4, S_5 are two distinct equilibrium-pairs, and each equilibrium-pair has the same local stable and unstable centre manifolds.

2.4. Four-wing chaotic attractor

Due to the asymmetry about the x-axis, z-axis and origin, the system (2) has more complex dynamical behaviours. Through numerical simulations, we find that the system can generate a four-wing chaotic attractor with wide parameter ranges. For example, when $a = 4$, $b = 6$, $c = 10$, $d = 5$, and $k = 1$, the proposed system has a four-wing chaotic attractor, and the equilibrium points are unstable. Figures 1(a)–1(c) are the phase portraits of the chaotic attractor.

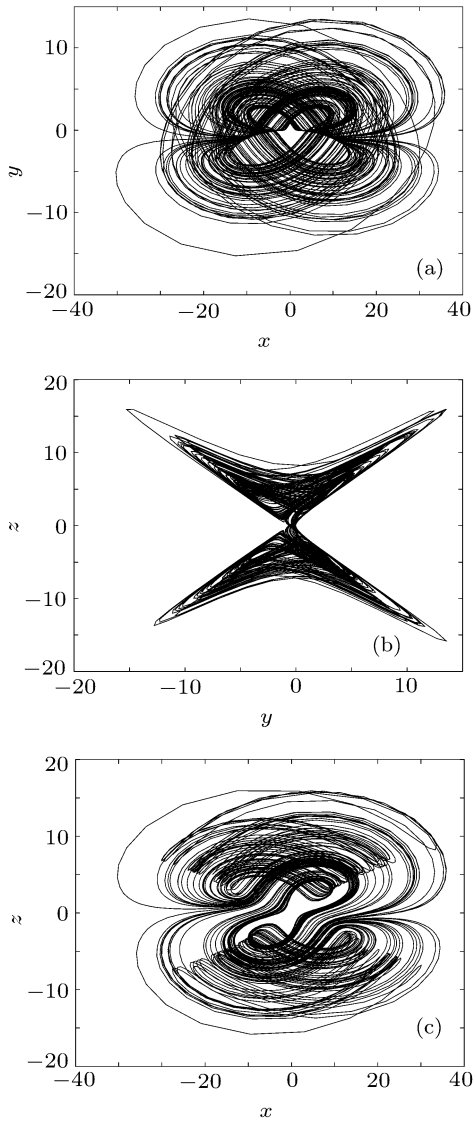


Fig.1. Four-wing chaotic attractor with $a = 4$, $b = 6$, $c = 10$, $d = 5$, $k = 1$. (a) Projection on $x - y$ plane, (b) projection on $y - z$ plane, (c) projection on $x - z$ plane.

3. Bifurcation analysis of the system

3.1. Hopf bifurcation analysis

The Jaccobian matrix of the proposed system is as follows:

$$\boldsymbol{J}(x^*, y^*, z^*) = \begin{bmatrix} a & -bz^* & -by^* \\ z^* & -c & x^* \\ k + y^* & x^* & -d \end{bmatrix}, \tag{13}$$

where x^*, y^*, z^* are the coordinates of the equilibrium points $S_1 - S_5$.

3.1.1. Hopf bifurcation analysis with respect to *a*

For the equilibrium point S_1, the characteristic equation is given by

$$\lambda^3 + (c+d-a)\lambda^2 + (cd-ac-ad)\lambda - acd = 0. \quad (14)$$

For $a > 0$, $b > 0$, $c > 0$, $d > 0, k > 0$, we have $-acd < 0$. By the Routh–Hurwitz stability criterion, Eq.(14) has eigenvalues with positive real part, thus the equilibrium point S_1 is unstable. The eigenvalues are $\lambda_1 = a$, $\lambda_2 = -c$, $\lambda_3 = -d$. Since the equilibrium point S_1 is a saddle point, it cannot undergo a Hopf bifurcation at equilibrium point S_1.

The characteristic equation at equilibrium point S_2 is given by

$$\lambda^3 + (c+d-a)\lambda^2 + \frac{1}{2a}(kc\sqrt{b^2k^2+4abd} - bck^2)\lambda + bck^2 + 4acd - kc\sqrt{b^2k^2+4abd} = 0. \quad (15)$$

By the Routh–Hurwitz stability criterion, when $c+d-a > 0$,

$$\frac{1}{2a}(kc\sqrt{b^2k^2+4abd} - bck^2) > 0,$$

$$bck^2 + 4acd - kc\sqrt{b^2k^2+4abd} > 0,$$

and

$$\begin{vmatrix} c+d-a & \frac{1}{2a}(kc\sqrt{b^2k^2+4abd} - bck^2) \\ bck^2 + 4acd - kc\sqrt{b^2k^2+4abd} & \end{vmatrix} > 0,$$

all the eigenvalues of Eq.(15) have negative real part thus the equilibrium point S_2 is stable. When Eq.(16) is satisfied, Eq.(15) has pure conjugate imaginary roots, and the system trajectory can evolve to a periodic orbit from a stable fixed point. Therefore, the system possesses a Hopf bifurcation.

$$\begin{vmatrix} c+d-a & \frac{1}{2a}(kc\sqrt{b^2k^2+4abd} - bck^2) \\ bck^2 + 4acd - kc\sqrt{b^2k^2+4abd} & \end{vmatrix} = 0. \quad (16)$$

When $b = 6$, $c = 10$, $d = 5$, $k = 1$, solving Eq.(16) gives $a = 2.2105$, and the eigenvalues of Eq.(15) are $\lambda_{1,2} = \pm 5.0684\mathrm{i}$, $\lambda_3 = -12.7895$. Obviously, a Hopf bifurcation arises at equilibrium point S_2 when $a = 2.2105$.

As S_2 and S_3 are an equilibrium-pair, the characteristic equation at S_3 is the same as Eq.(15). Therefore, a Hopf bifurcation arises at S_3.

From Fig.2(a), we obtain that this Hopf bifurcation process is in the forward direction. Figures 2(b)–2(c) show that the system trajectory can evolve to a periodic orbit from a stable fixed point as a increases from 1 to 2.5.

The characteristic equation at equilibrium point S_4 is described as

$$\lambda^3 + (c+d-a)\lambda^2 - \frac{1}{2a}(kc\sqrt{b^2k^2+4abd} + bck^2)\lambda + bck^2 + 4acd + kc\sqrt{b^2k^2+4abd} = 0. \quad (17)$$

By the Routh–Hurwitz stability criterion, when $a > 0$, $b > 0$, $c > 0$, $d > 0$, $k > 0$, the equilibrium point S_4 is stable if the condition

$$(c+d-a) > 0,$$

$$-\frac{1}{2a}(kc\sqrt{b^2k^2+4abd} + bck^2) > 0,$$

and

$$bck^2 + 4acd + kc\sqrt{b^2k^2+4abd} > 0$$

are satisfied. But

$$-\frac{1}{2a}(kc\sqrt{b^2k^2+4abd} + bck^2) > 0$$

is not satisfied in the system parameters range, thus equilibrium point S_4 is a saddle point, and the Hopf bifurcation cannot arise. Since S_4 and S_5 are an equilibrium-pair, the same holds for equilibrium point S_5.

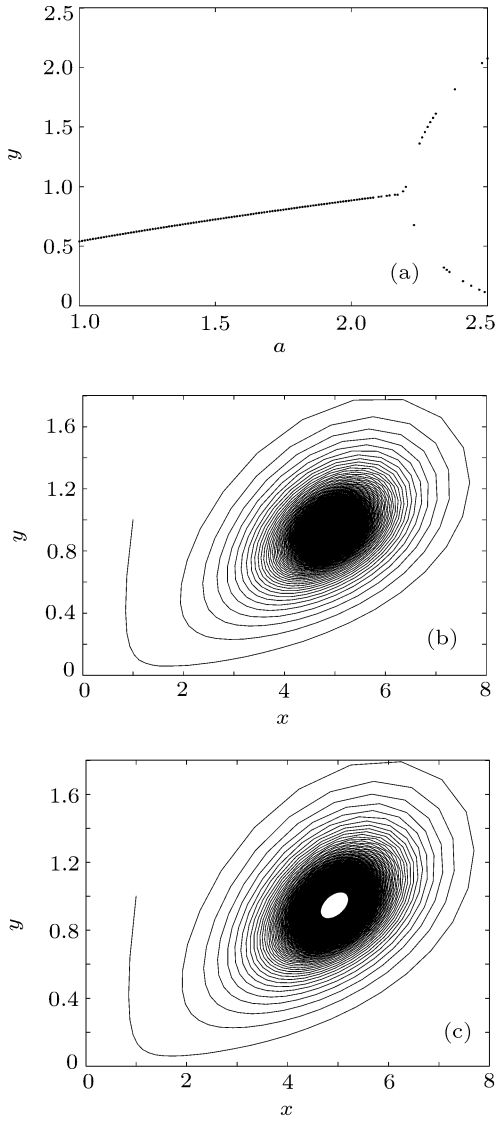


Fig.2. Hopf bifurcation analysis with respect to a. (a) Hopf bifurcation process versus a, with $b = 6$, $c = 10$, $d = 5$, $k = 1$; (b) phase portrait for $a = 2.205$; (c) phase portrait for $a = 2.2105$.

3.1.2. Hopf bifurcation analysis with respect to k

By using the same method, the Hopf bifurcation process with k can be studied. For example, fixing $a = 4$, $b = 6$, $c = 10$, $d = 5$, we find that a Hopf bifurcation arises at equilibrium points S_2 and S_3 when $k = 3.8962$. As shown in Fig.3(a), this bifurcation process is in the backward direction. Figures 3(b) and 3(c) show that the system trajectory can evolve from a fixed point into a periodic orbit with decreasing k.

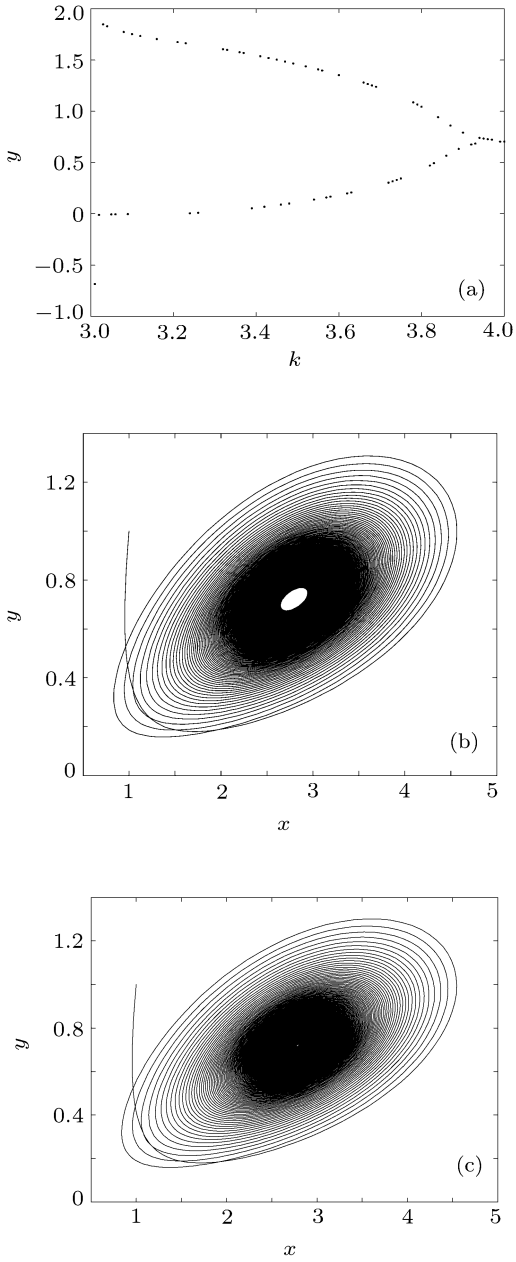


Fig.3. Hopf bifurcation analysis with k. (a) Hopf bifurcation process versus k, with $a = 4$, $b = 6$, $c = 10$, $d = 5$; (b) phase portrait with $k = 3.8962$; (c) phase portrait with $k = 3.9162$.

3.2. Numerical bifurcation analysis

For a chaotic system, its basic dynamical properties can be illustrated by numerical bifurcation diagram and Lyapunov exponent spectrum.

3.2.1. Numerical bifurcation analysis with respect to a

We fix $b = 6$, $c = 10$, $d = 5$, $k = 1$, and vary parameter a. As shown in Fig.4(a), the system has complex dynamical behaviours as a increases from 1 to 7; the system trajectory evolves into a chaotic attractor from a fixed point, finally into a periodic orbit. There are three periodic windows [3.65, 3.83], [4.29, 4.45], and [4.89, 4.93] in the bifurcation diagram.

In this sub-section, Lyapunov exponents are calculated by the Gram–Schmidt algorithm.[22] As shown in Fig.4(b), when $a \in [1, 2.2105)$, the Lyapunov exponents L_1, L_2 and L_3 are smaller than zero, indicating that the system is asymptotically stable. When $a \in [2.2105, 2.82]$, the largest Lyapunov exponent L_1 is equal to zero, which implies that the system is periodic. Obviously, when $a = 2.2105$, a Hopf bifurcation emerges. The largest Lyapunov exponent L_1 is greater than zero when $a \in [2.82, 5.49]$ except in periodic windows, which implies that the system is chaotic. The system is periodic when $a \in (5.49, 7]$.

Figures 5(a)–5(d) show the periodic orbits on the $x - y$ plane when a is in different periodic windows, and Fig.5(e) shows that a four-wing chaotic attractor is generated when $a = 5$.

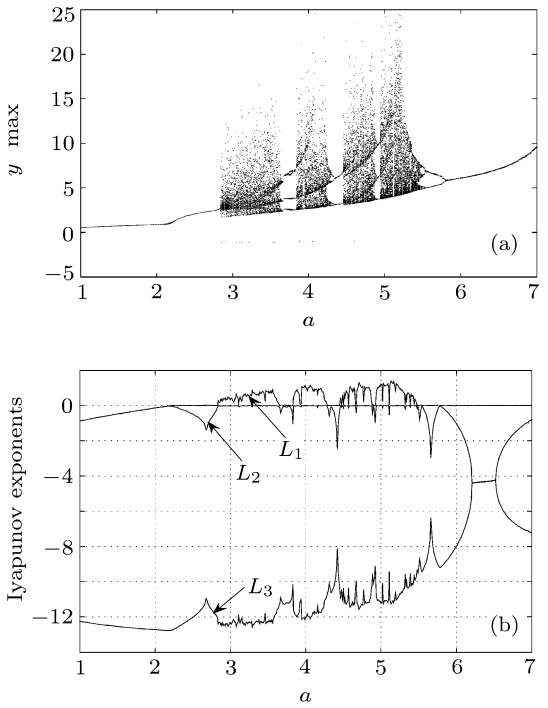


Fig.4. Numerical bifurcation analysis with respect to a, with $b = 6$, $c = 10$, $d = 5$, $k = 1$. (a) Bifurcation diagram versus a, (b) Lyapunov exponent spectrum versus a.

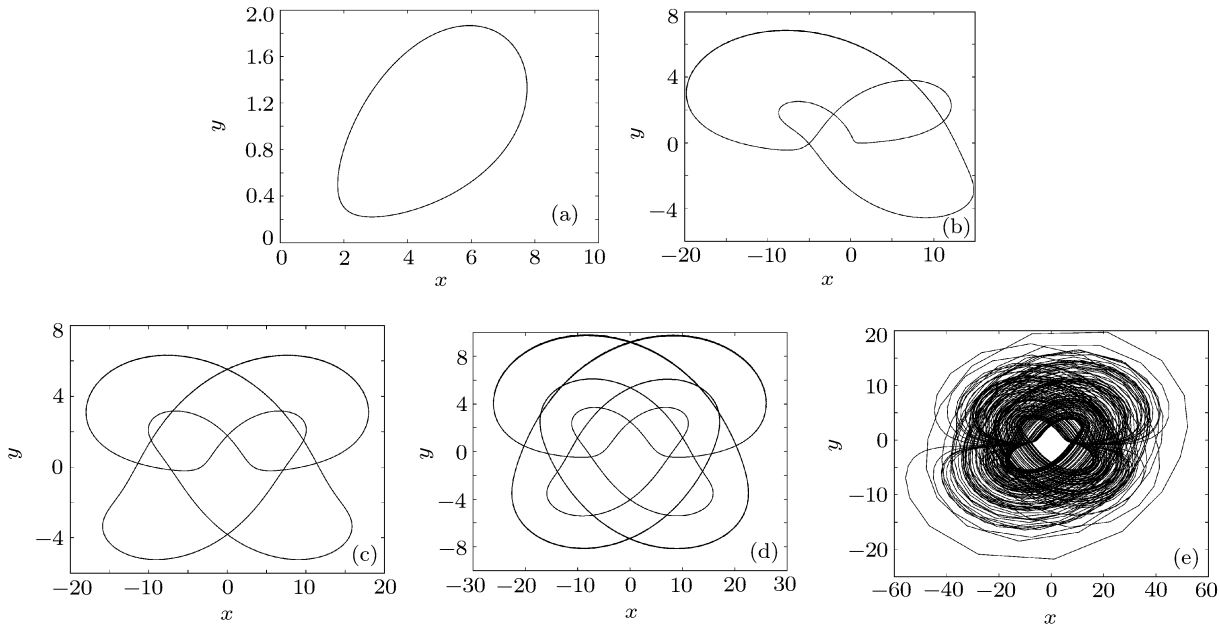


Fig.5. Phase portraits on $x - y$ plane with $b = 6$, $c = 10$, $d = 5$, $k = 1$. (a) Periodic orbit with $a = 2.4$, (b) periodic orbit with $a = 3.8$, (c) periodic orbit with $a = 4.4$, (d) periodic orbit with $a = 4.9$, (e) chaotic attractor with $a = 5$.

3.2.2. Numerical bifurcation analysis with respect to k

We fix $a =$, $b = 6$, $c = 10$, $d = 5$, and vary parameter k. As shown in Fig.6(a), as k increases from 0 to 4, the system trajectory evolves into a periodic orbit from the chaotic attractor, and finally into a fixed point. There are four obvious periodic windows in the bifurcation process. By observing Fig.6(b), the four periodic windows are [0.09, 0.18], [0.45, 0.48], [0.62, 0.78] and [1.21, 1.26].

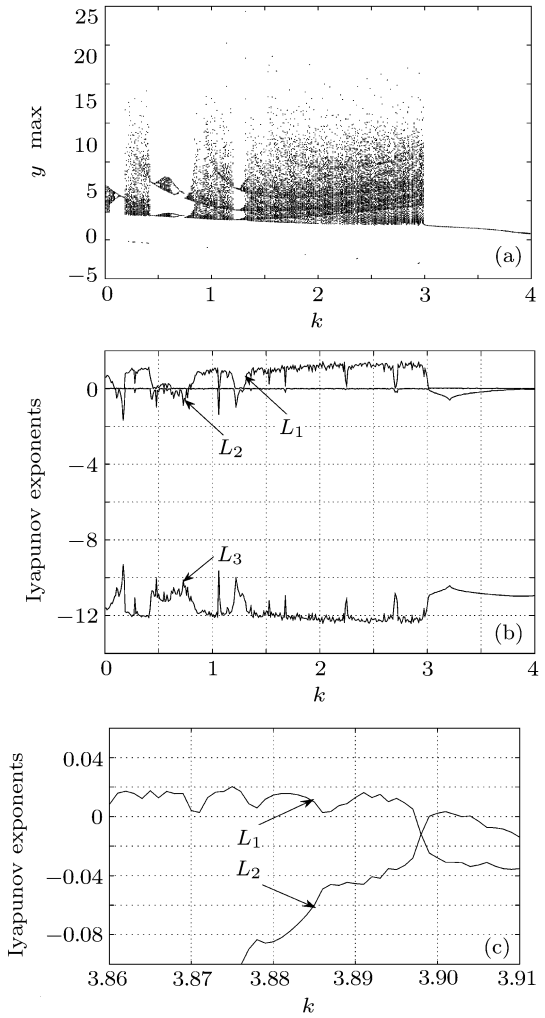


Fig.6. Numerical bifurcation analysis with respect to k, with $a = 4$, $b = 6$, $c = 10$, $d = 5$. (a) Bifurcation diagram, (b) Lyapunov exponent spectrum, (c) partly enlarged view of Lyapunov exponents.

As shown in Fig.6(b), the system is chaotic when $k \in [0, 3.01]$ except in periodic windows. Figures 7(a)–7(c) show the different periodic orbits when k is in corresponding periodic intervals. Figure 7(d) shows that a four-wing chaotic attractor is generated when $k = 2$.

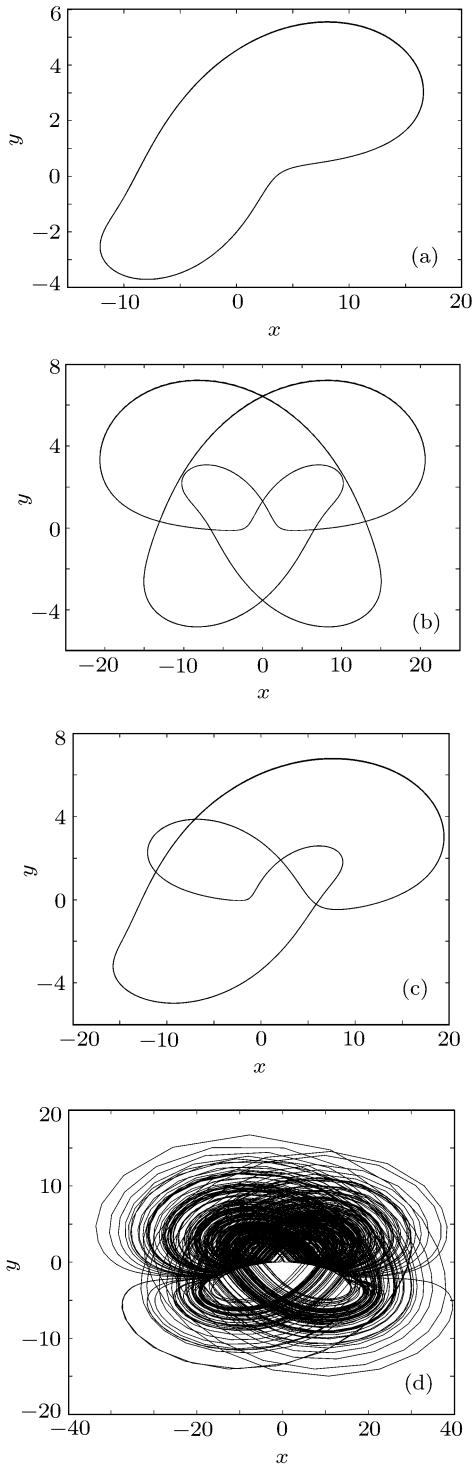


Fig.7. Phase portraits on $x - y$ plane with $a =$, $b = 6$, $c = 10$, $d = 5$. (a) Periodic orbit with $k = 0.16$, (b) periodic orbit with $k = 0.46$, (c) periodic orbit with $k = 1.21$, (d) chaotic attractor with $k = 2$.

Based on the Hopf bifurcation analysis, the largest Lyapunov exponent L_1 is smaller than zero when $k > 3.8962$. As shown in Fig.6(c), the largest Lyapunov exponent L_1 is also smaller than zero when $k > 3.8962$, and $L_1 \approx 0$ when $k = 3.8962$. Considering the tiny calculation error, the numerical simulation is in agreement with the Hopf bifurcation analysis.

4. Circuit design and realization

To physically realize the four-wing chaotic system, an analog circuit is designed. As shown in Fig.8, the circuit consists of three channels to realize the integration, addition and subtraction of the state variables x, y and z, respectively. The operational amplifier TL082 and its peripheral circuit can realize the additive operation, invert operation, integral operation; the analog multiplier AD633 can realize the nonlinear product operation. For this type of realization, the corresponding state equations are given by

$$\begin{aligned}
\dot{x} &= \frac{R_2}{R_3R_{14}C}x - \frac{R_2}{R_1R_{14}C}yz,\\
\dot{y} &= \frac{R_{11}}{R_{12}R_{14}C}y - \frac{R_{11}}{R_{10}R_{14}C}xz,\\
\dot{z} &= \frac{R_5R_8}{R_4R_9R_{14}C}x - \frac{R_5R_8}{R_6R_9R_{14}C}z + \frac{R_8}{R_7R_{14}C}xy.
\end{aligned} \tag{18}$$

Obviously, the state variables x, y and z in Eq.(18), correspond to the state voltages of three channels respectively. If we take system parameters $a = 4$, $b = 6$, $c = 10$, $d = 5$, $k = 1$, then we have $R_1 = 50$ kΩ, $R_2 = 30$ kΩ, $R_3 = 75$ kΩ, $R_4 = 50$ kΩ, $R_5 = 5$ kΩ, $R_6 = 10$ kΩ, $R_7 = 100$ kΩ, $R_8 = 10$ kΩ, $R_9 = 10$ kΩ, $R_{10} = 100$ lΩ, $R_{11} = 10$ kΩ, $R_{12} = 10$ kΩ, $R_{13} = 1$ kΩ, $R_{14} = 100$ kΩ, $C = 1$ μF.

With these circuit elements, the state voltages of the circuit (18) are about 50 V. Considering the saturation property of the analog multipliers and the operational amplifier, we reduce the state variables of the system (2) fivefold under linear transformation to avoid saturation distortion, thus the system model is transformed to

$$\begin{aligned}
\dot{x} &= 4x - 30yz,\\
\dot{y} &= -10y + 5xz,\\
\dot{z} &= x - 5z + 5xy.
\end{aligned} \tag{19}$$

Accordingly, fixing the other circuit element values, we have $R_1 = 10$ kΩ, $R_7 = 20$ kΩ, $R_{14} = 20$ kΩ. To obtain the stable phase portrait in the oscilloscope, we adjust the capacitor C from 1 μF to 470 pF, which does not change the shape of the phase portrait but only increases the vibration frequency of the chaotic circuit. Thus, the stable phase portraits are observed in the oscilloscope. As shown in Figs.9(a)–9(e), the phase portraits observed in the experimental setup are in agreement with those by the numerical simulation.

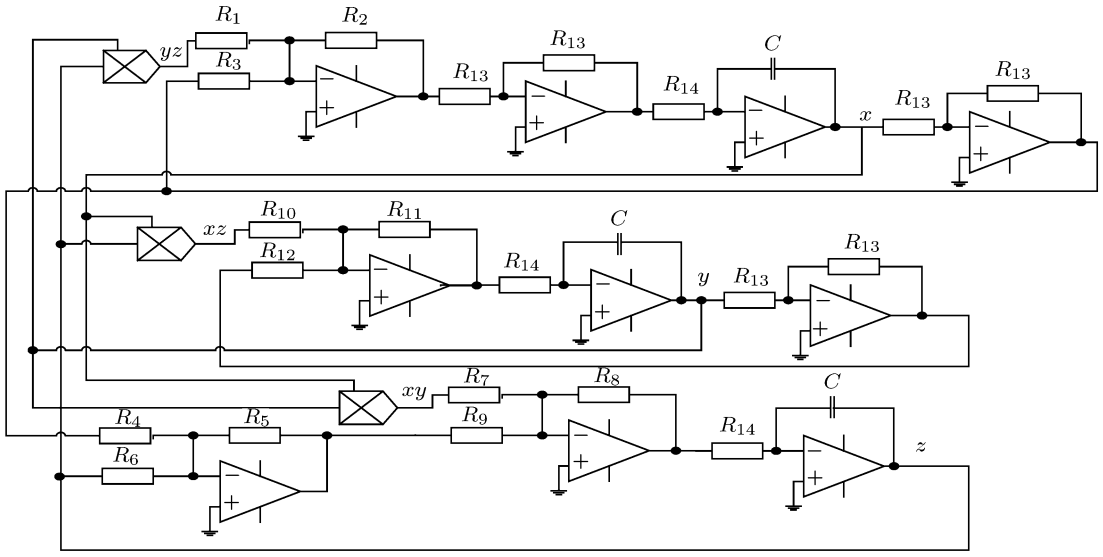


Fig.8. Circuit realization of the four-wing chaotic system.

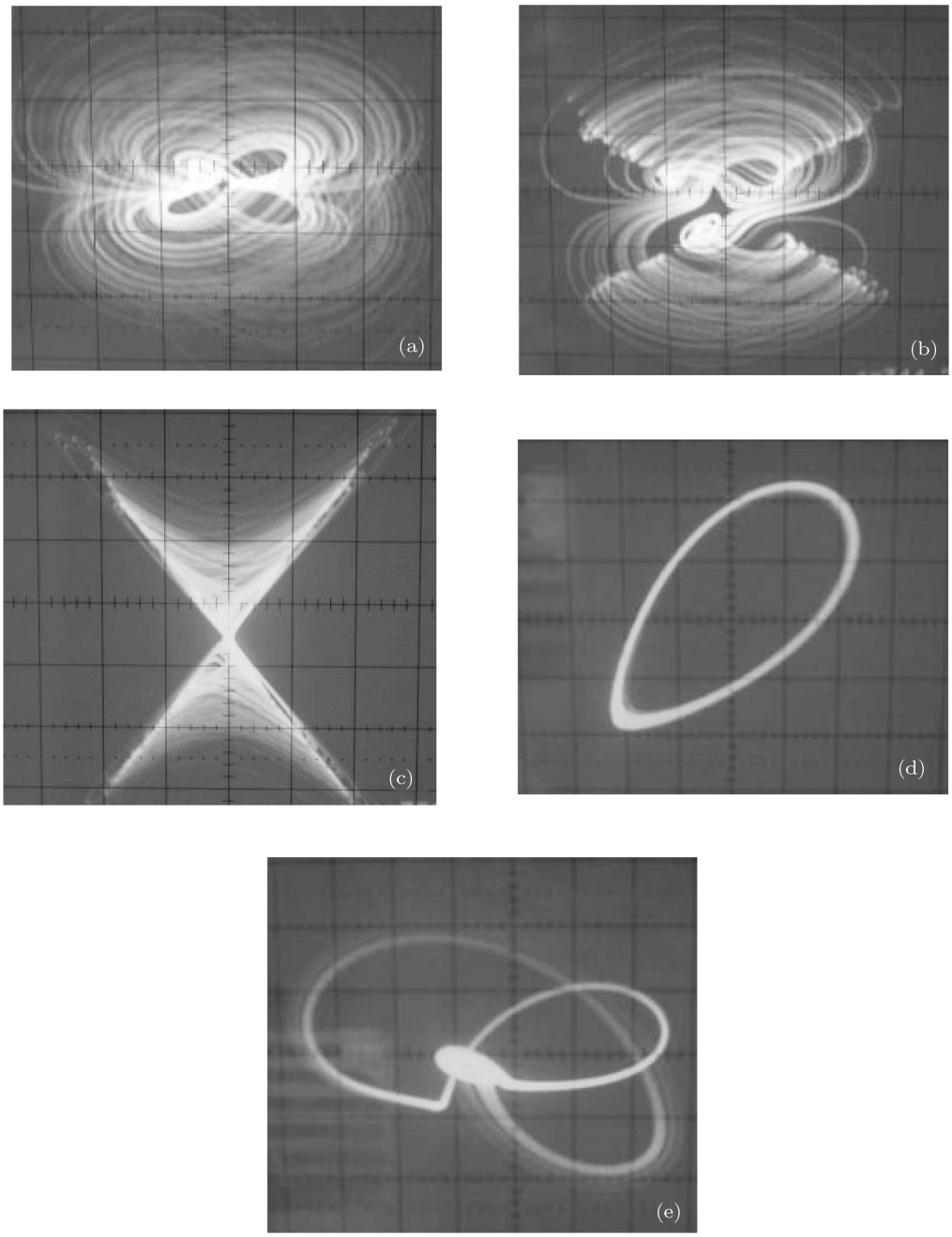


Fig.9. Phase portraits of system (19) observed in the experimental setup. (a) Chaotic attractor on $x-y$ plane, (b) chaotic attractor on $x-z$ plane, (c) chaotic attractor on $y-z$ plane, (d) periodic orbit on $x-y$ plane with $a=2.4$, (e) periodic orbit on $x-y$ plane with $a=3.8$.

5. Summary

A new four-wing chaotic attractor has been generated from a 3D autonomous chaotic system in this paper; the chaotic system contains five parameters and three quadratic cross-product terms. The Hopf bifurcation processes are proved to arise at certain equilibrium points through theoretical analysis. Numerical bifurcation analysis shows that the system has interesting complex dynamical behaviours. Finally, an analog circuit is designed to physically realize the four-wing chaotic system; the result of circuit realization is in agreement with that of the numerical analysis. The existence of the four-wing chaotic attractor is verified by the analog circuit realization. For its simple algebraic structure and complex dynamical behaviour, the proposed system is useful in secure communication.

References

[1] Lorenz E N 1963 *J. Atmos. Sci.* **20** 130

[2] Li T Y and Yorke J A 1975 *Amer. Math. Monthly* **82** 985

[3] Ott E, Grebogi C and Yorke J A 1990 *Phys. Rev. Lett.* **64** 1196

[4] Zhang Y H, Qi G Y, Liu W L and Yan Y 2006 *Acta Phys. Sin.* **55** 3307 (in Chinese)

[5] Chen Z Q, Yang Y, Qi G Y and Yuan Z Z 2007 *Phys. Lett.* A **360** 696

[6] Liu C X 2007 *Acta Phys. Sin.* **56** 6865 (in Chinese)

[7] Song Y Z, Zhao G Z and Qi D L 2007 *Control Theory Application* **24** 795 (in Chinese)

[8] Chen G R and Mao Y B 2004 *Chaos, Solitons and Fractals* **21** 749

[9] Sun L and Jiang D P 2006 *Acta Phys. Sin.* **55** 3283 (in Chinese)

[10] Song Y Z, Zhao G Z and Qi D L 2006 *Chin. Phys.* **15** 2266

[11] Chen G and Ueta T 1999 *Int. J. Bifur. Chaos* **9** 1465

[12] Lu J H and Chen G 2002 *Int. J. Bifur. Chaos* **12** 659

[13] Lu J H, Chen G, Cheng D and Celikovsky S 2002 *Int. J. Bifur. Chaos* **12** 2917

[14] Qi G Y, Chen G R, Du S Z, Chen Z Q and Yuan Z Z 2005 *Phys.* A **352** 295

[15] Liu C X, Liu L, Liu T and Li P 2006 *Chaos, Solitons and Fractals* **28** 1196

[16] Li W L and Song Y Z 2008 *Acta Phys. Sin.* **57** 51 (in Chinese)

[17] Wang F Q, Liu C X and Lu J J 2006 *Acta Phys. Sin.* **55** 3289 (in Chinese)

[18] Liu W B and Chen G 2003 *Int. J. Bifur. Chaos* **13** 261

[19] Liu W B and Chen G 2004 *Int. J. Bifur. Chaos* **14** 1395

[20] Chen Z Q, Yang Y and Yuan Z Z 2008 *Chaos, Solitons and Fractals* **38** 1187

[21] Qi G Y, Chen G R, M A Wyk B J Wyk and Zhang Y H 2008 *Chaos, Solitons and Fractals* **38** 705

[22] Alan Wolf, Jack B S, Harry L S and John A V 1985 *Phys.* D **16** 285

[23] Arfken G 1985 *Mathematical Mettods for Physicists* 3rd ed (Orlando, FL: Academic Press) p516